University of Tennessee, Knoxville
TRACE: Tennessee Research and Creative Exchange

Senior Thesis Projects, 2007 College Scholars

2007

Nucleoside Analogs as Anti-HIV Compounds and Phosphorylation of the Prodrug with NDP Kinase: A Molecular Modeling Study and a Synthetic Route

Shawn Robertson

Follow this and additional works at: https://trace.tennessee.edu/utk_interstp4

Recommended Citation

Robertson, Shawn, "Nucleoside Analogs as Anti-HIV Compounds and Phosphorylation of the Prodrug with NDP Kinase: A Molecular Modeling Study and a Synthetic Route" (2007). *Senior Thesis Projects, 2007.*
https://trace.tennessee.edu/utk_interstp4/10

This Project is brought to you for free and open access by the College Scholars at TRACE: Tennessee Research and Creative Exchange. It has been accepted for inclusion in Senior Thesis Projects, 2007 by an authorized administrator of TRACE: Tennessee Research and Creative Exchange. For more information, please contact trace@utk.edu.

FORM C
COLLEGE SCHOLARS PROJECT APPROVAL

Shawn Robertson — Scholar

Dr. John Turner — Mentor

Nucleoside Analogs as Anti-HIV compounds and Phosphorylation of the prodrug with NDPKinase: A Mol. Mod. Study and Synthetic Route

Project Title

COMMITTEE MEMBERS
(Minimum 3 Required)

Name	Signature
George K. Schweitzer	Geo. K. Schweitzer
JOHN TURNER	John Turner.
DAVID C. BAKER	David C. Baker

PLEASE ATTACH A COPY OF THE SENIOR PROJECT TO THIS SHEET AND RETURN BOTH TO THE PROGRAM DIRECTOR. THIS PAGE SHOULD BE DATED AND COMPLETED ON THE DATE THAT YOUR DEFENSE IS HELD.

DATE COMPLETED 4/18/07

Nucleoside Analogs as Anti-HIV Compounds and Phosphorylation of the Prodrug with NDP Kinase: A Molecular Modeling Study and a Synthetic Route

College Scholars Senior Project

Presented for the

Bachelor of Arts

Degree

The University of Tennessee, Knoxville

Dr. Baker
Dr. Turner
Dr. Schweitzer

Shawn Robertson

April 2007

ABSTRACT

Undergoing anabolic phosphorylation by intracellular kinases to form nucleoside triphosphates, nucleoside reverse transcriptase inhibitors (NRTIs), are the leading antiretroviral agents for the treatment of human immunodeficiency virus. Phosphorylation rates of the endogenous nucleosides and their corresponding analogs are governed by intracellular and extracellular factors. A total synthesis and molecular dynamic study of didanosine is presented to gain insight into the differences in phosphorylation between endogenous nucleosides and their analogs.

Introduction

Human immunodeficiency virus (HIV) is a retrovirus and the formative cause of acquired immunodeficiency syndrome (AIDS). Reverse transcriptase is an RNA-dependent DNA polymerase that converts viral RNA (+) to a form, DNA, which can be incorporated into the host's genome. The two leading therapeutic families of inhibitors of reverse transciptase are the non-nucleoside inhibitors (NNRTIs) and the nucleoside inhibitors (NRTIs). NNRTIs work by binding to RT and bring about a change in the binding pocket. They are targeted at allosteric sites of reverse transcriptase, i.e, at nonsubstrate binding sites. NRTIs, as the name indicates, are biochemical variations of the "normal" or endogenous nucleosides produced inside the cell. They must be phosphorylated by a combination of intracellular enzymes to their active triphosphate (TP) forms in order to be used as a substrate in DNA synthesis. Once they are converted to their active TP form, they compete with the proviral DNA substrates for binding sites on reverse transcriptase and act as chain terminators if incorporated into nascent viral DNA.[1] The nucleoside analogs are specific to reverse transcriptase inhibiton and have minimum inhibitory effects on other DNA polymerases. There are some toxic effects that may arise due to inhibition of γ–DNA polymerase in mitochondria. Approved NRTIs are orally bioavailable and have a short serum half-life, yet their intracellular half-life is relatively longer.[1] FDA-approved compounds that resemble both endogenous purine and pyrimidine nucleosides include abacavir (ABC), tenofovir disoproxil (PMPA), zidovudine (ZDV), stavudine (d4T), lamivudine (3TC), salcitabine (ddC), and didanosine (ddI).[2] All of these compounds act as chain terminators due to the lack of a 3'-hydroxyl group on the ribose ring.

Nucleoside Analogs are Prodrugs

Kinases are enzymes that facilitate in the transfer of a phosphoryl group from adenosine triphosphate (ATP) to an acceptor. There are numerous types of acceptors because phosphorylation is used by many biological processes. Nucleoside diphosphate kinase (NDPK) is a very important enzyme to take into consideration when dealing with the development of antiretroviral treatments (NRTIs) due to their lack of 3'-OH groups on the ribose rings of nucleoside analogs.[3] Antiviral analogs are generally considered to be phosphorylated by the same series of cellular kinases as those that act on the natural nucleotides. Activation of analogs into the mono- and diphosphate forms is orchestrated by nucleoside kinases and nucleoside monophosphate kinases. This is accompolished with various degrees of specificity, i.e, purine analogs are phosphorylated under a different set of enzymes and conditions than pyrimidines.[4] In contrast though, activation to the triphosphate form is achieved by NDP kinase, which is nonspecific for the nucleobase moiety of the donor and acceptor nucleotide. It has previously been mentioned that the 3'-OH on the ribose ring plays an important role in the phosphorylation mechanism of NDP kinase. Reasons for this could be due to hydrogen-bond formation between the gamma phosphate and the 3'-OH or donation of a proton to the phosphate group.[5] If considered a vital role in the mechanism, it could account for the reason why dideoxy nucleotide analogs like ddI-DP are phosphorylated at such a low rate. The phosphorylation mechanism for purine analogs and the associated enzymes necessary for purine metabolism are discussed in this paper.

Steps for Phosphorylation

Just like endogenous nucleosides, NRTIs make use of the nucleotide synthesis and phosphorylation pathways in the host cell. The route to the diphosphate form varies between the two different groups of nucleosides, purine and pyrimidine, yet the last step in the pathway, shared by most endogenous nucleosides and NRTIs, is catalyzed by nucleoside diphosphate kinase. Purine metabolism is more complicated and complex than pyrimidine metabolism due to the fact that it must go through numerous extra steps involving adenylate kinase and other enzymes. The deoxyadenosine analog didanosine is an analog of the purine nucleoside inosine. For the case of the prodrug 6-Cl-ddP, it is transformed to the active drug, ddI, by the enzyme adenosine deaminase (Scheme 1).

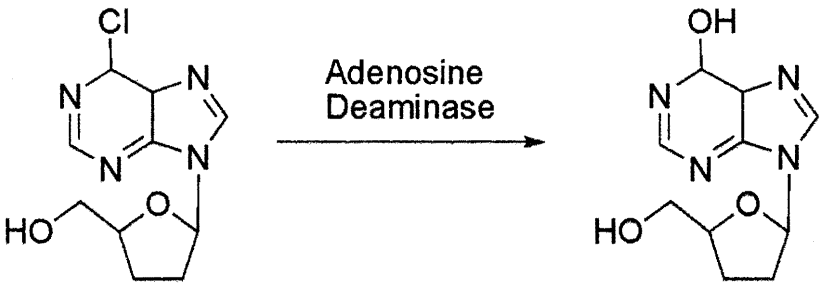

Scheme 1. Transformation of 6–ClddP to 2'-3'-ddI.

Once the monophosphate ddI has been formed, the adenylate phosphorylation pathway may continue.[6] There are many enzymes used to convert ddI to dideoxyadenosine monophosphate and all have been indentified.[7, 8] However all the necessary enzymes required in the phosphorylation of ddA-MP to ddA-TP have not yet been fully characterized but assumed to be adenylate kinase and nucleoside diphosphate kinase.[6]

Structure of Nucleoside Diphosphate Kinase

The structure of nucleoside diphosphate kinase was realized through the crystal structure obtained by Janin et al.[9] The cartoon of the structure follows in Figure 1.

Figure 1. Crystal Structure of subunit of nucleoside diphosphate kinase.

There are approximately 150 amino acid residues that make up the enzyme nucleoside diphosphate kinase. As with most proteins, NDP kinases are oligomeric, and in eukaryotes the enzymes are homohexamers. There is an α/β domain, consisting of about 90 residues that form the core of the subunit. The core represents a four-stranded anti-parallel β-sheet and two connecting α-helixes. The strand order comprising the β-sheet is $\beta_2\beta_3\beta_1\beta_4$. β_1 is connected to β_2 by the helix α_1, while helix α_3 connects strands β_3 to β_4. The β-sheet, along with its two connecting α-helixes, characterize a structural configuration often times known as an $\alpha\beta$ sandwich, or $\beta\alpha\beta\beta\alpha\beta$ fold, or simply the ferrodoxin fold. The ferrodoxin fold is very common to many proteins. This structural element derived its name from its first observation in *Pseudomonas aerogenes*

ferrodoxin. As the α-helixes pack onto the β-sheets, a well-maintained hydrophobic core is created. Strands β_1 and β_3 are located in the middle of the sheet and are very hydrophibic, as evident by the amino acid residues. In order to extend the hydrophobic core to other subunits, strand β_2 has a leucine-rich sequence which forms a "β-strand leucine zipper". This effectively promotes dimerization and burries the β_2 strand in the hydrophobic core even though it is an edge strand in the individual subunit. The majority of these proteins have one side of the beta-sheet covered by the two connecting α helixes, while the other side remains open. This is not the case for nucleoside diphosphate kinase. In NDP kinase both sides of the β-sheet are covered. As mentioned previously, the bottom side is covered with the α-helixes 1 and 3, while the top is enshrouded by a pair of helixes, α-A-α-2, which is a hairpin centrally located betweens strands β_2, β_3 and helix α_4. The active site of NDP kinase is a histidine residue located at position 122 on the β_4 strand. It is positioned on the perimeter of the beta sheet and allows it to remain exposed for phosphorylation. Finalization of the subunit fold is accompolished by the addition of the Kpn loop and C-terminal segment. The Kpn loop is 22-residues in length, 96–117, and separates α_3 and β_4. Consisting of the last 20 residues, (134–152) in NDP Kinase B, the C-terminal segment is the final part of the subunit occurring after helix α_4. The quaternary structure of the enzyme is very different between classes of organisms. In eukaryotes NDP kinase occurs as a hexamer, while in prokaryotes it is a tetramer (as in *Myxoccus*). The hexamer has a 70-Å diameter and a 50-Å thickness. Its dihedral D3 symmetry can be viewed as three trimers related by symmetry. Two subunits can dimerize by beta-sheet extension to essentially form an eight-stranded antiparallel beta-sheet. The residues that make contact are located on

helix α_1, strand β_2, and between residues 140 and 145 of the C-terminal segment. At each dimer interface, there are approximately 10–12 hydrogen bonds. The Kpn loop and C-terminal residues 149–152 are the greatest donors to the trimer interface. The reason for this is because the tip of the loop is in close proximity to the threefold axis of the hexamer. In its entirety, six Kpn loops come together, three on the top face and three on the bottom, to confine a cavity composed of roughly 100 water molecules. A fissure forms on the protein surface at the binding site about 20 Å long, 6 Å wide, and 10 Å deep. At the bottom of the fissure, His118 can be resolved. The mechanisms of binding of NDP kinase is all together different from that of a "classic" convention as seen in protein kinases such as adenylate kinase, ATPase, GTPase , and nucleoside monophosphate kinase. NDP kinase appears to have an anomalous binding mechanism. β_4 is a short four-residue strand that contains the active-site residue, His118, and is found immediately following the Kpn loop. A requisite for the loop to be connected to the β-strand is a positive psi angle of residue 116. This residue is very often an isoleucine in most eukaryotes. The side chain of isoleucine should seem disinclined to form a positive psi angle due to its branching, yet this is what is seen experimentally. This pattern is essential to the function of the enzyme because had Ile116 a β-strand conformation, the branched side chain would act as a hindrance and block the approach of the incoming nucleotide substrate from the imidazole group. A hydrogen bond from the NH of Ile 116 to the side chain of Asp 14 conserves this unfavorable conformation. The N atom of the catalytic imidazole group of histidine can interact with the carboxylate of Glu129. This is not the only residue that Glu129 can interact with. Ser120, a residue in close proximity to the catalytic histidine on the β-strand, is involved in a His–Glu–Ser triad. The His118

residue acts as a nucleophile, and the Glu129 residue acts as a base. The job of Glu129 is to keep the imidazole group in the proper position as well as to keep the N protonated. The binding site on the enzyme will acknowledge ribose and 2'-deoxyribose, as well as other known nucleobases. The bound nucleotide is found between the αA–α2 hairpin and the Kpn loop. The base is located in proximity to the surface of the protein while the phosphate groups are contained within the enzyme and are angled towards the active-site residue. Comparing different protein structures with bound substrates shows that the base can move by 3–4 Å depending on which base is used. This proves that the job of the binding site is to fit an array of groups. The sugar is located inside the bound enzyme complex away from the protein surface and has many polar interactions. The 2'-OH and 3'-OH of ribose can hydrogen-bond to the amino group of Lys 12 and to the amide group of Asn 115. If the 2'-OH is missing, as in deoxyribose, a water molecule can take its place and have a minimal effect on the overall binding energy. The sugar assumes a C3'-*endo* ring puckering, which directs the base into the *anti*-position . This is not the only conformation that the binding pocket accepts. In order for dideoxyribose to bind, the sugar must assume a different ring pucker. The β-phosphate folds back towards the sugar and forms a hydrogen bond with the sugar 3'–OH. The oxygen is a leaving group when the active-site residue is phosphorylated by a nucleotide triphosphate, and by microreversibility, an attacking group when the active site is dephosphorylated by a nucleotide diphosphate. This bond makes the connecting oxygen of the β and γ phosphate much more reactive. It is shown to be very important due to the low activity of dideoxynucleotides. These analogs are phosphorylated 10^4–10^5 times less efficiently than other substrates.[9]

Cellular Factors Affecting Phosphorylation

A large number of nucleoside diphosphate kinases are presented in the cell.[10] The turnover of the enzyme is very high, greater than 1000 s^{-1}, so therefore even a poor substrate will eventually be phosphorylated.[11]. There are some cellular factors that can affect the rate of phosphorylation and have nothing to do with the substituent on or missing from the 3'–position of the ribose ring. Metabolism may vary by cell type because different cell types are associated with different efficiencies of cellular kinases. Phosphorylation rates may be affected by the ddNTP:dNTP ratio present in the host cell. Common sense would predict a higher ratio of ddNTP to have a greater antiviral effect and result in greater inhibition of reverse transcriptase.[7] Another factor affecting the phosphorylation rate of the nucleoside is the activation state of the cell. The phosphorylating activity varies in resting vs. stimulated cells for the different nucleosides. The final factor which could affect the rate of phosphorylation is the infection status of the cell. Whether or not the phosphorylation ability of an infected cell is altered from that of a non-infected cell is unknown. It is speculated that there would be higher dNTP levels in HIV-infected individuals rather than uninfected ones.[6]

Effective Treatment for Aids Dementia

In order to treat AIDS dementia there must be increased concentrations of dideoxynucleoside analogs delivered to the brain where the AIDS virus has penetrated the central nervous system (CNS). Didanosine (2',3'-dideoxyinosine, ddI) was the second NRTI approved for treatment by the FDA. As promising as the drug appeared, it had several delivery-related disadvantages.[12] It had a highly variable bioavailability, but

more importantly, a low central nervous system uptake. The ability to construct antiviral agents that cross the central nervous system has become a daunting task due to the prevalence of the AIDS dementia complex, a progressive deterioration in mental capacity accompanying AIDS patients.[13] Since dideoxynucleosides are not very lipophilic, they penetrate the central nervous system very poorly.[14] There was a need for a prodrug that was inactive, yet capable of being altered back to the original active form by some enzyme-catalyzed reaction. The compound should address the lipophilicity problems and problems associated with crossing the CNS which plagued the original NRTIs. The optimal lipophilicity will correlate to the ideal intestinal absorption and membrane permeability. While achieving a high CNS penetration rate is advantageous, ones does not want to have too high of a rate to avoid passive diffusion across the blood–brain barrier.[15] A solution to crossing the blood–brain barrier and increasing the concentration of the ddN reaching the CNS came about by going through a series of adenosine deaminase-actived 6-halo-dideoxypurine prodrugs.[16] Adenosine deaminase is present in a 10-fold higher concentration in the brain than in blood plasma[16]. 6-Chloro-9-(2,3-dideoxy-β-D-*glycero*-pentofuranosyl)purine (6-ClddP) provided a 10-fold increase in concentration of delivery of ddI to the brain parenchyma compared to ddI controls[16]. This effective increase in concentration can be attributed to the increased lipophlicity of 6-ClddP and to its conversion to ddI inside the brain. As stated earlier, this conversion is realized with the use of the enzyme, adenosine deaminase (Scheme 1).[12] The mechanism of conversion is nucleophilic aromatic substitution where a water molecule in the active site of the enzyme is the nucleophile. 6-ClddP crosses the blood–brain barrier with much more efficiency than ddI because it is roughly 30 times more lipophilic.

Modeling Approach

Since the 2' and 3'-OHs are missing from the nucleotides, there is going to be a change in conformation upon binding. There have been several crystal structures obtained for the enzyme, including itself in the free state, the phosphorylated intermediate, and the enzyme complexed with endogenous nucleosides such as ADP and GDP.[17] Unfortunately there have been no crystal structures obtained for the enzyme complexed with dideoxypurine nucleosides. The γ-phosphate of a nucleoside triphosphate is transferred by NDP kinase through a phosphohisitdine intermediate onto a nucleoside diphosphate.[18] Human nucleoside diphosphate kinase complexed with ADP was modeled using SYBYL 7.2 on a Silicon Graphics workstation using the Tripos forcefield. Utilizing the crystallographic data from protein data bank number 2HVD, and incorporating the methods of Hutter et al,[3] a model of the active site was set up for the computational investigation of the enzyme NDP kinase. The residues considered in vicinity of the active His 118 and ADP included: Glu 129, Lys 12, Asn 115, Val 112 and Phe 60 (Figure 2).

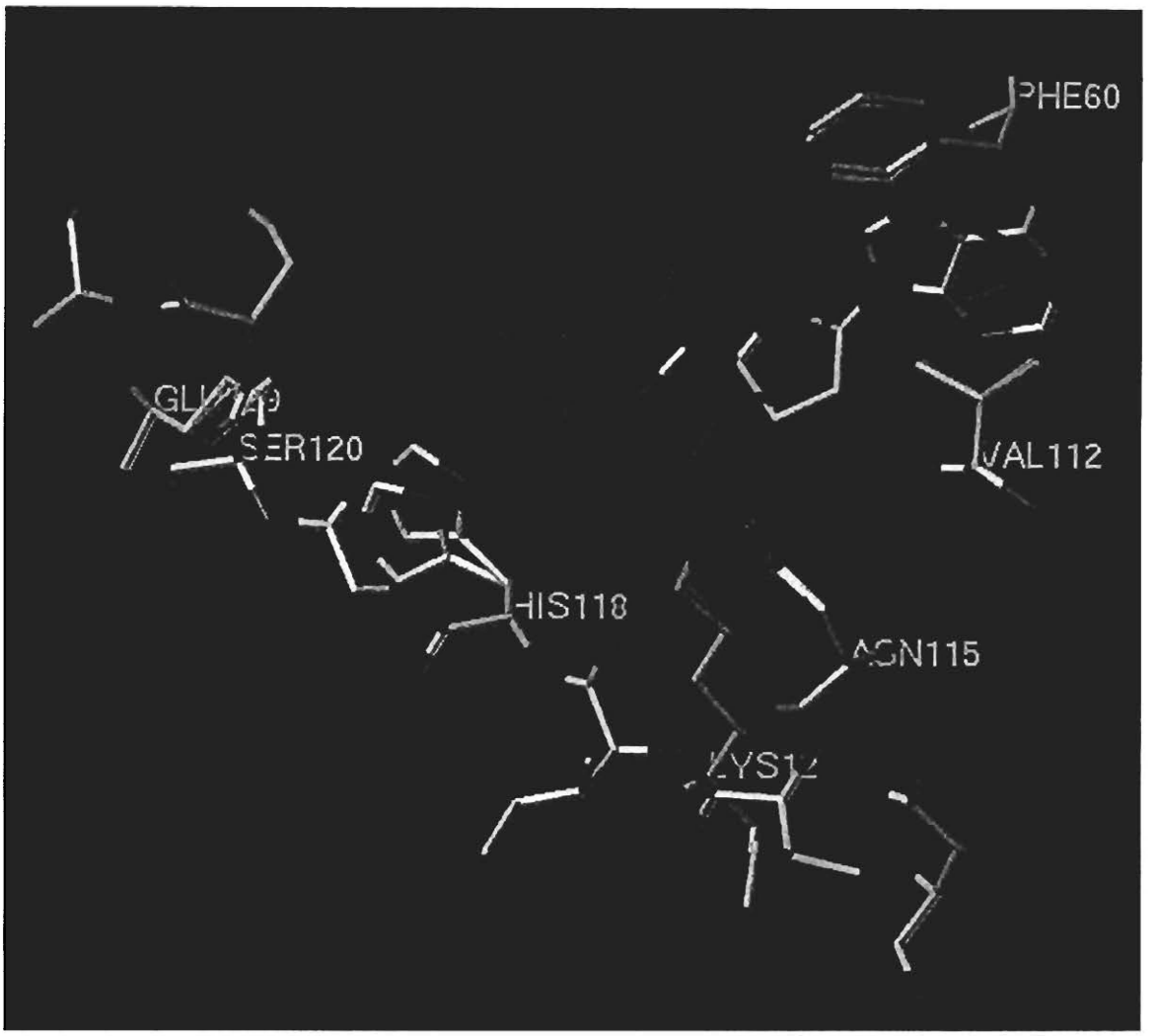

Figure 2. Binding pocket of NDP kinase for nucleoside with labeled residues. Hydrogen atoms were added prior to the computation to ensure that all side chains remained protonated. See Table 1 for a listing of key interactions of ddI DP complexed with the enzyme.

Key interactions of ddI DP complexed with NDPK	*Key interactions of ADP complexed with NDPK*
β-phosphate oxygen hydrogen bond with His 118 2.67 Å	2' and 3'-OH H-bond to Lys 12 and Asn 115

Hydrogen bond between Glu 129 and Ser 120	His-Glu-Ser triad (as described earlier)
Lys 12 and Asp 115 hydrogen bond	This interaction is not seen
Intramolecular bonding between phosphate atoms	No intramolecular bonding between phosphate
π stacking between Phe 60 and nitrogenous base 3.98 Å	Val 112 and Phe 60 encompase the base as it sits in the binding pocket

Table 1. Key interactions of ddI DP complexed with NDP kinase

Discussion of Modeling

SYBYL predicted a hydrogen bond from the beta phosphate oxygen to the catalytic His 118, which was not seen on the original ADP enzyme complex (Figure 3).

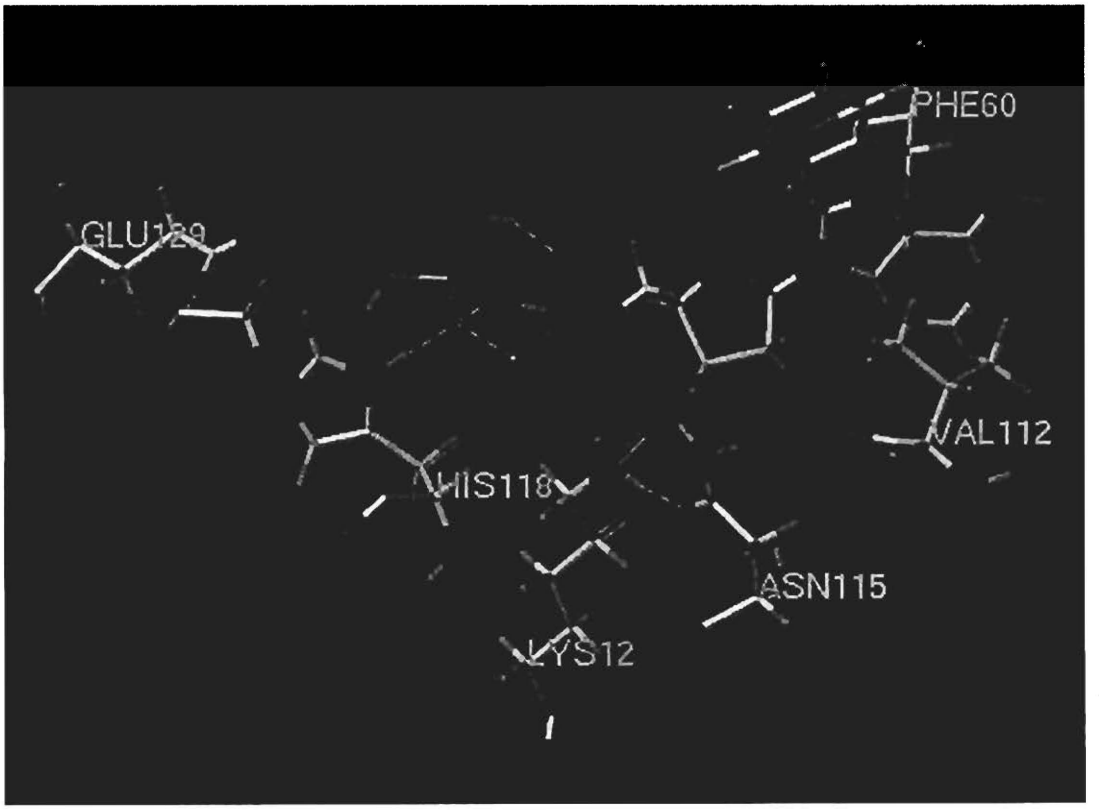

Figure 3. SYBYL predicted H-bonds with bound ddI DP.

Intramolecular bonding of the phosphates of ddI was also shown as a possibility after acquisition using Tripos forcefield. Other important interactions analyzed were the hydrophobic ones that involved π stacking between the nitrogenous bases, Phe60, and Val112. In the ADP enzyme complex Val112 and Phe60 incompases the base, and the distance between the center of the base and the center of Phe 60 is less than 3.5 Å. In contrast, Val112 has no interaction between ddI, and Phe60 is shifted to produce a 3.98 Å π stacking interaction between the two ring systems.

Synthesis of 6-chloro-9-(2,3-dideoxy-β-D-*glycero*-pentofuranosyl)purine

The D-*glycero*-pentofuranose ring system is synthesized from commercially available L-glutamic acid. The reaction can be considered to involve a diazotization by interaction of N_2O_3 (HNO_2) with the amino group on L-glutamic acid. This leads to the formation of a diazonium ion, a good leaving group. (Scheme 2).

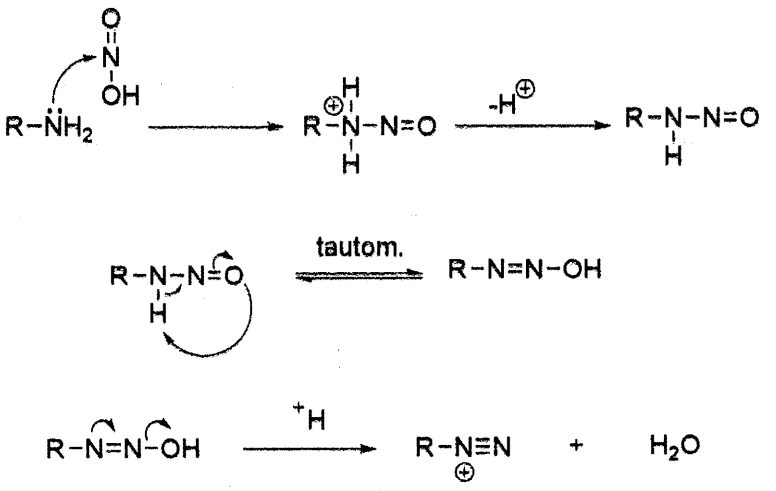

Scheme 2. Carbocation intermediate of N-nitrosation.

A sensible mechanism that would produce (*S*)-(+)-carboxy-γ-butyrolactone very rapidly would be one where the γ-carboxyl group acts as a nucleophile. (Scheme 3).

Configuration will be preserved due to the neighboring-group participation effect of the adjacent α-carboxyl group. Once the cyclic carbonium ion is formed, simple deprotonation would yield the lactone (Scheme 3).

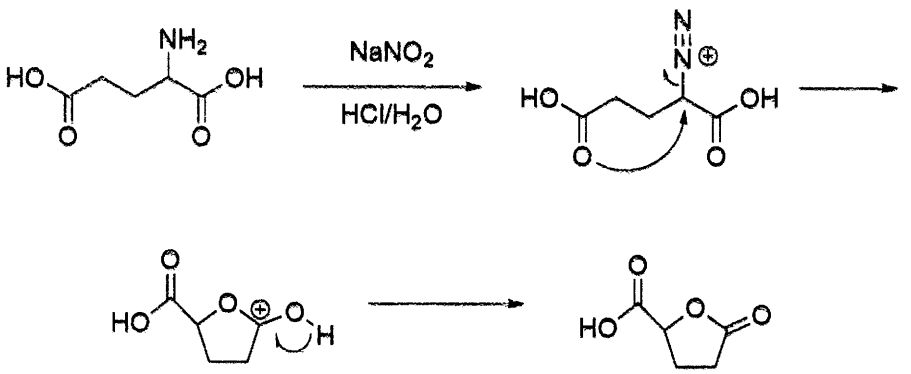

Scheme 3. Synthesis of (*S*)-(+)-Carboxy-γ-butyrolactone.

BH_3, a strong Lewis acid, is used as the reducing reagent for the carboxylic acid on the above lactone. It is an electron acceptor and can interact with lone pairs of electrons or nucleophiles. Diborane does not exist as free BH_3 but rather as the diborane dimer B_2H_6 or complexed with a Lewis base. Diborane shows numerous differences in its reducing power than those portrayed by the alkali metal borohydrides. During the early 1960s carboxylic acids were normally considered to be relatively resistant to reducing agents, but this all changed with the introduction and commercial availability of diborane, which converts carboxylic acids to the corresponding alcohols very rapidly.[20] It is a very versatile reducing agent because it produces high yields with ease of isolation of products over a variety of functional groups. Methylsulfide·borane (DMSB) is advantageous in this case over the use of borane·THF (BTHF) complex for two reasons. Firstly DMSB is not as reactive as BTHF due to the stronger coordination of borane to Me_2S. This assures that DMSB will not over-reduce the ring. Secondly DMSB is very

stable and can be produced and used in high concentrations. The first step in the reduction is the formation of triacylborane. Since the electron deficiency of the boron atom exerts a powerful demand on the lone pairs of the acyl oxygen, the resonance that occurs is between the boron atom and the oxygen atom rather than the carbonyl group as proposed by Brown et al.[20] (Scheme 4).

Scheme 4. Resonance between boron and oxygen atoms

that the carbonyl groups of the triacylboranes now resemble those of aldehydes or ketones more closely than those of esters (Scheme 5).[20]

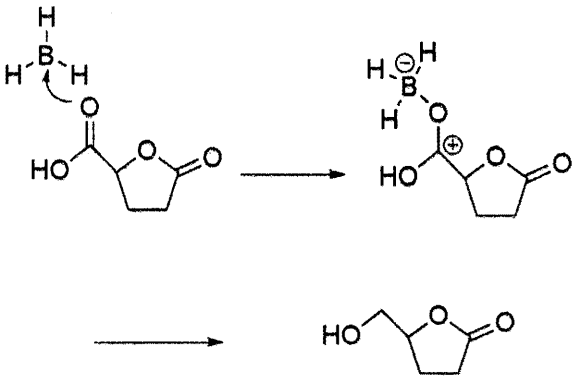

Scheme 5. Synthesis of (*S*)-(+)-Hydroxymethyl-γ-butyrolactone.

Protection of the hydroxyl groups via silyl ethers is very important to synthetic organic chemistry. The general order of stability of the protection groups towards acidic media are TMS (1) < TES (64) < TBS (20,000) < TIPS (700,000) < TBDPS (5,000,000)

and the stability towards basic media is TMS (1) < TES (10-100) < TBS ~ TBDPS (20,000). The *tert*-butyldiphenylsilyl (TBDPS) moiety was chosen as the protecting group because the reaction is run in base, and it allows one to monitor reaction progress since, when absorbed onto a TLC sheet, the TBDPS moiety absorbs UV light. This reaction is catalyzed by 4-dimethylaminopyridine (4-DMAP) because it is a powerful electron-donating group and aids in the formation of a charged intermediate.[21] Once the charged intermediate is formed, the reaction proceeds similar to that of a Williamson ether synthesis following an S_N2 fashion (Scheme 6).

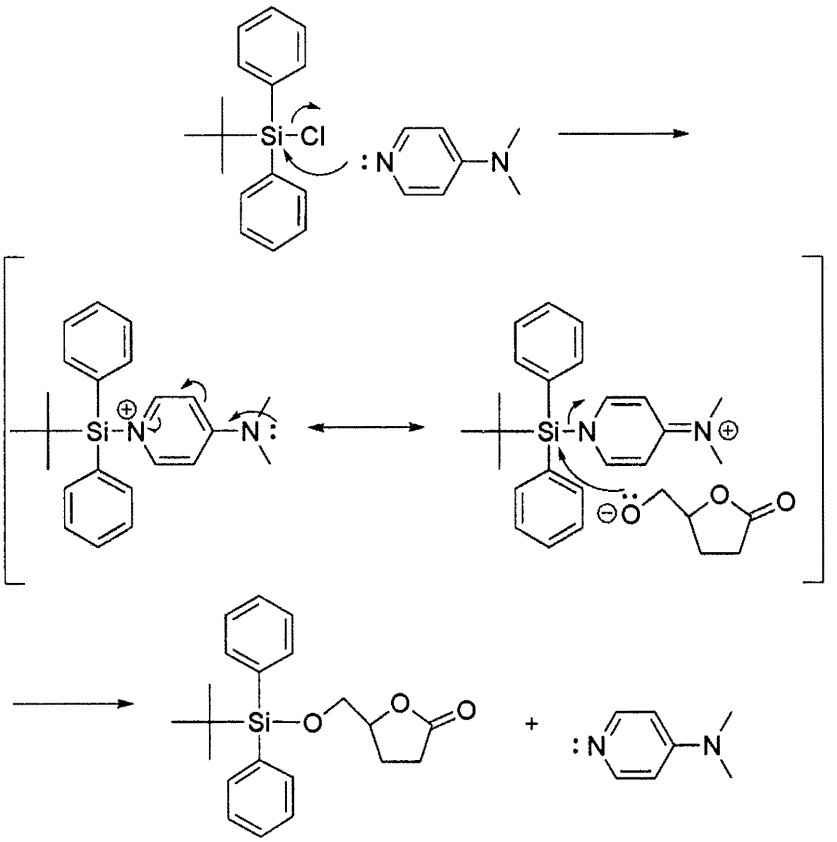

Scheme 6. Synthesis of S-(+)-*tert*-butyldiphenylsilyloxymethyl-γ-butyrolactone

During the next stage in the synthesis, the lactone, a cyclic ester, is reduced to a lactol. Over-reduction is prevented by the hemiacetal functionality that essentially "masks" the aldehyde. Diisobutylaluminumhydride (DIBAL-H) is the reducing reagent and used at -78 °C to prevent over-reduction. A proposed mechanism follows in Scheme 7.

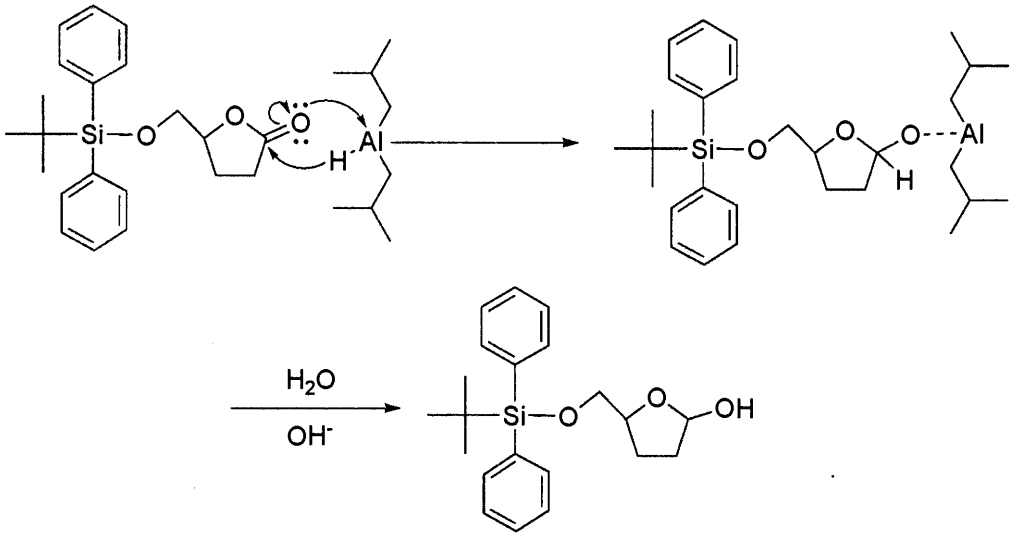

Scheme 7. Synthesis of 5-*O*-*tert*-butyldiphenylsilyl-2,3-dideoxy-D-*glycero*-pentofuranose.

During the coupling step of the synthesis, the anomeric hydroxyl group is converted to a trifluoroacetyl ester. This group is a very good leaving one—much better than the hydroxyl group. The trifluoroacetyl group is very reactive, and thus the reaction must take place at -40 °C and under strictly anhydrous conditions. The trifluoroacetyl ester and 6-Cl purine group are safe in basic media, so pyridine is a logical choice as the catalyst. An oxonium ion is formed, and the coupling reaction can proceed by a mechanism that is somewhere in between an S_N1 and S_N2 reaction[15] (Scheme 8).

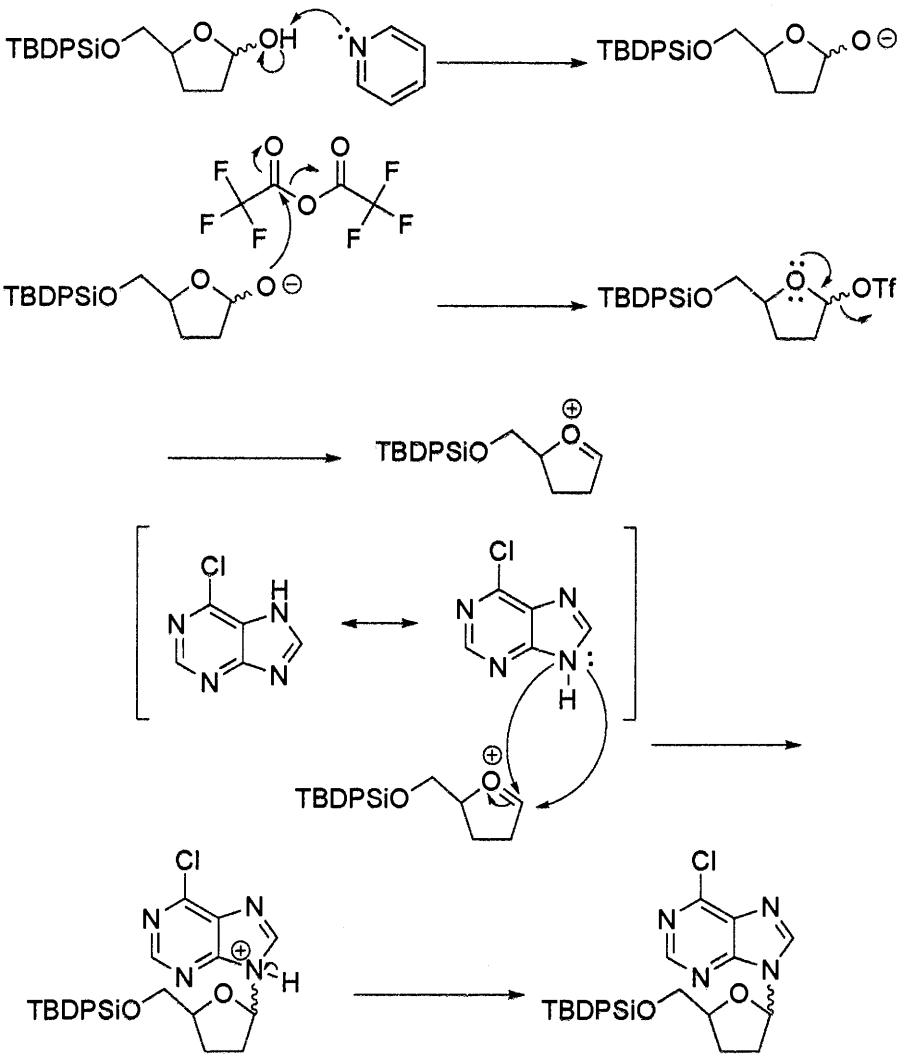

Scheme 8. Synthesis of 6-chloro-9-[5-*O*-(*tert*-butyldiphenylsilyl)-2,3-dideoxy-β-D-*glycero*-pentofuranosyl]purine.

The final step in the synthesis is the deprotection of the *tert*-butyldiphenylsilyl group. This is achieved by tetrabutylammonium fluoride (TBAF) (Scheme 9).

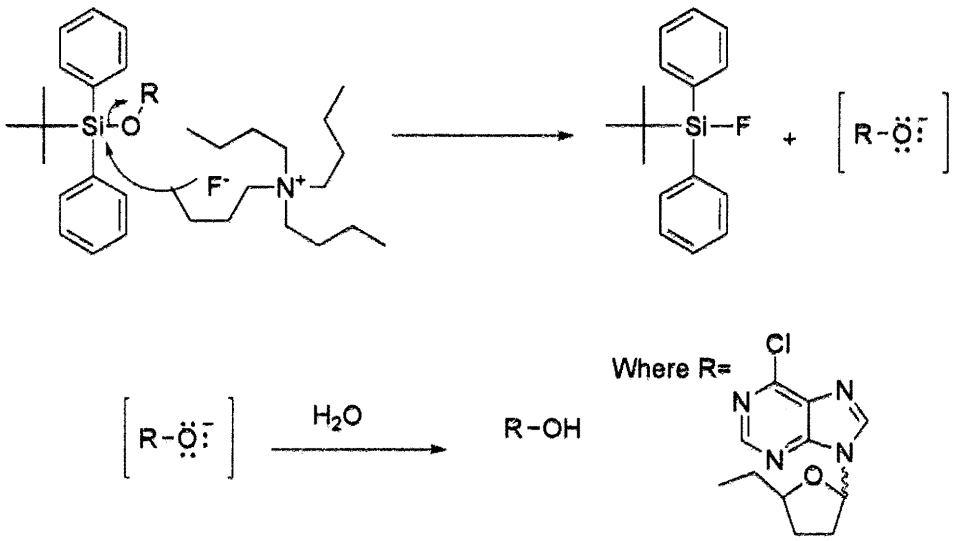

Scheme 9. Synthesis of 6-chloro-9-(2,3-dideoxy-β-D-*glycero*-pentofuranosyl)purine.

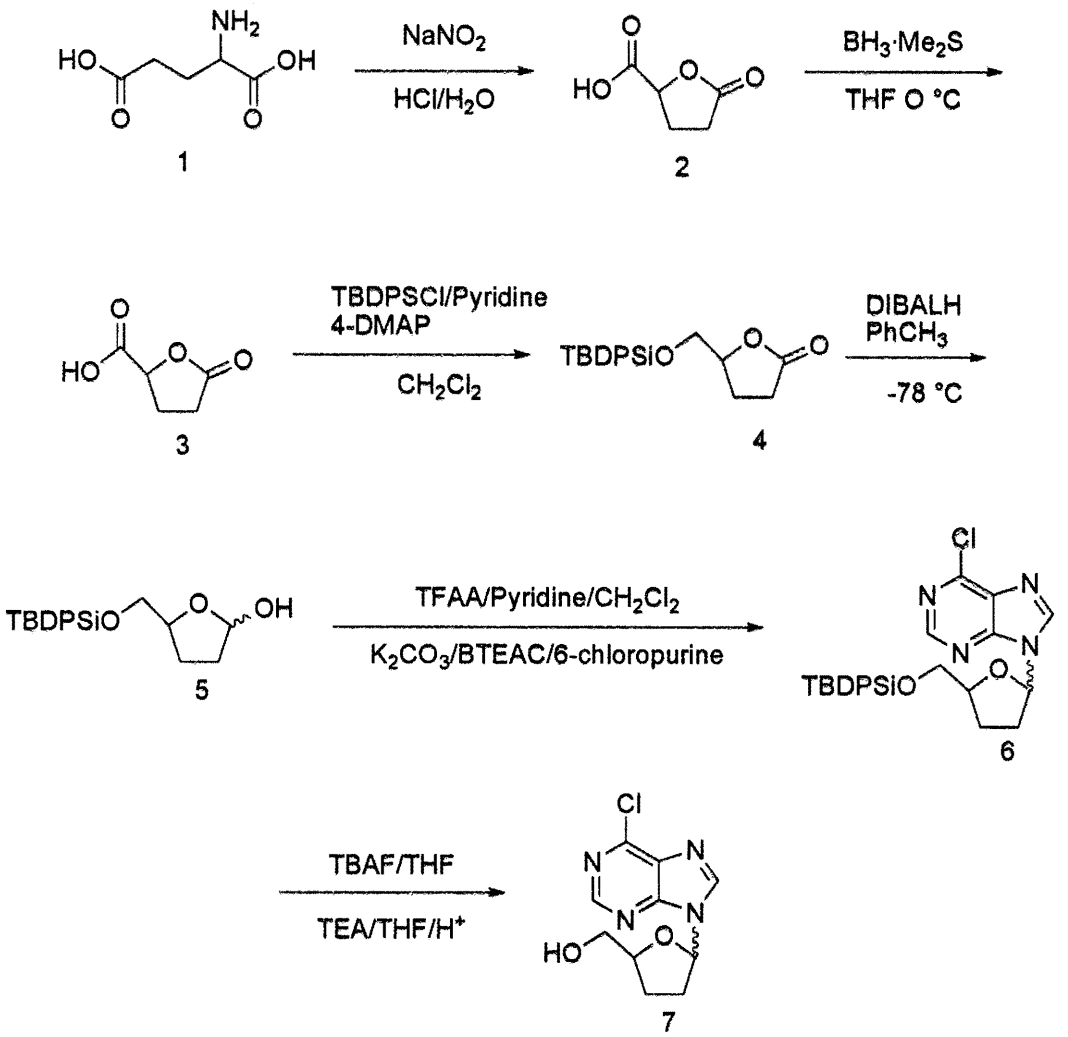

Experimental

A. General Methods

All solvents and reagents used for this synthetic approach were reagent grade. The solvents were anhydrous and dried as follows: dichloromethane (CH_2Cl_2), pyridine, toluene, and acetonitrile (CH_3CN) were distilled from calcium hydride; tetrahydrofuran (THF) was dried over sodium-benzophenone ketyl and distilled. All solvents were prepared fresh and stored in clean, dry glassware in a desiccator prior to use. After reactions were complete, excess solvents were evaporated using a Büchi rotary evaporator and a warm water bath with temperatures no higher than 40 °C. There were

some evaporations carried out at very low pressures, and these made use of a high-vacuum rotary evaporator. Reaction progress was monitored by TLC on aluminum-backed plates. Products were separated using column chromatography, which was achieved using coarse 70–230 Mesh ASTM silica gel. The TLC plate was visualized under UV light of 254-nm and also by dipping in anisaldehyde–sulfuric acid in ethanol, followed by a short blast of heat from a heat gun.

B. Preparation of Compounds

Synthesis of (*S*)-(+)-Carboxy-γ-butyrolactone (2)

A suspension of L-glutamic acid (**1**, 50 g, 0.34 mol) in concentrated HCL (72 mL) and H_2O (130 mL) was cooled to -5 °C in a round-bottom flask. To this suspension was added dropwise over a period of 3 h a solution of sodium nitrite ($NaNO_2$, 35 g, 0.50 mol) in H_2O (75 mL). It is very important that the temperature be kept at -5 °C during the entire addition. The reaction was slowly warmed to room temperature and allowed to stir for 48 h. The water was evaporated with the use of a high-vacuum rotary evaporation apparatus and a warm water bath of 50 °C. The product was freeze-dried using a bench-top lyophilizer which converted the yellowish syrup into a white-yellow solid. The solid was extracted with EtOAc (200 mL), suction filtered, and dried over anhyd $MgSO_4$. After the $MgSO_4$ was filtered from the product, the EtOAc was rotary evaporated and the product dried under high-vacuum, resulting in a yellowish syrup that was further dried in a drying pistol (CH_2Cl_2 reflux) for 48 h to produce the product **2** (30.6 g, 235 mmol, 61.2%) as a pale-yellow solid.

Physicochemical data: ^{1}H NMR ($CDCl_3$, 300 MHz): δ 2.3–2.73 (m, 4H, H-2 and H-3), 4.97 (m, 1H, H-4), 9.8 (bs, 1H, H-5), [Lit.[22] CD_3OD, 100 MHz): 1.8–2.3 (m, 4H, H-2 and H-3), 4.2 (m, 1H, H-4)]

Synthesis of (*S*)-(+)-Hydroxymethyl-γ-butyrolactone (3)

To a solution of (S)-(+)-carboxy-γ-butyrolactone (**2**, 5.0 g, 38 mmol) in anhyd THF (20 mL) at -78 °C (dry–ice–acetone bath) was added a solution of 2 M borane·methyl sulfide complex in THF (22 mL, 44.2 mmol) over the period of 1 h under a nitrogen atmosphere. The temperature of the addition was kept at -78 °C. The mixture was stirred for 5 h at -78 °C with constant monitoring of the temperature and cooling when required. The reaction mixture was quenched by cautiously adding dry MeOH (20 mL) at -78 °C, and the product was coevaporated with methanol three times. After high-vacuum rotary evaporation, the product was placed on the high-vacuum pump overnight and dried to produce **3** (3.95 g, 34 mmol, 79%) as a pale-yellow oil.

Physicochemical data: bp 125–135 °C/high-vacuum, (Lit.[22] 131–147 °C/7mm); ^{1}H NMR data ($CDCl_3$, 300 MHz): δ 2.05–2.75 (m, 4H, H-2 and H-3), 3.6–3.95 (m, 3H, H-5 and H-6), 4.58–4.68 (m, 1H, H-4), [Lit.[22] (100 MHz) 2.0–2.8 (m, 4H, H-2 and H-3) 3.6–4.0 (m, 3H, H-5 and H-6), 4.65 (m, 1H, H-4)].

Synthesis of **(*S*)-(+)-*tert*-Butyldiphenylsilyloxymethyl-γ-butyrolactone (4)**

A solution of (S)-(+)-hydroxymethyl-γ-butyrolactone (**3**, 3.9 g, 34 mmol), 4-dimethylaminopyridine 4-DMAP (0.1 g, 0.8 mmol), and pyridine (2 mL, 25 mmol) was dissolved in dry CH_2Cl_2 (40 mL) at room temperature under anhydrous conditions and under a nitrogen atmosphere. To this mixture was added *tert*-butyldiphenylsilyl chloride TBDPS-Cl (10.6 mL, 40.8 mmol) dropwise over the course of 1 h. The reaction mixture

was allowed to stir for 24 h at room temperature and was further refluxed for 3 h; reaction progress was monitored by TLC. The reaction mixture was allowed to cool to room temperature where it was washed with H_2O (2 × 25 mL). After the organic layer was separated it was dried over anhyd $MgSO_4$ to remove any residual water, producing a yellow–brown syrup. Column chromatography, with an eluent consisting of hexane–CH_2Cl_2, followed by an increasing ratio of dichloromethane, was used to purify the syrup. The desired fractions were collected, and the product was recrystallized from hexane to yield **4** (8.2 g, 23.12 mmol, 68%).

Physicochemical data: R_f 0.35 (4:1 CH_2Cl_2-hexane); ^{1}H NMR data ($CDCl_3$, 300 MHz): δ 0.98–1.05 (s, 9H, *tert*-butyl), 2.1–2.75 (m, 4H, H-2 and H-3), 3.63–3.89 (2dd, 2H, H-5), 4.55–4.65 (m, 1H, H-4), 7.35–7.7 (m, 10H, phenyl), [Lit.[23] (250 MHz) δ 1.0–1.1 (s, 9H, *tert*-butyl), 2.1–2.8 (m, 4H, H-2 and H-3), 3.6–3.9 (2dd, 2H, H-5), 4.5–4.7 (m, 1H, H-4), 7.3–7.8 (m, 10H, phenyl).

Synthesis of 5-*O*-*tert*-butyldiphenylsilyl-2,3-dideoxy-*D*-*glycero*-pentofuranose (5)

(*S*)-(+)-*tert*-butyldiphenylsilyloxymethyl-γ-butyrolactone (**4**, 5.0 g, 14 mmol) was dissolved in dry $PhCH_3$ (50 mL) in a dry round-bottom flask with a dry stir bar under a nitrogen atmosphere. The flask and its contents were cooled to -78 °C (dry–ice–acetone bath) and was added cautiously diisobutylaluminumhydride DIBAL-H (15.2 mL, 1.2 M $PhCH_3$, 18.4 mmol) over the course of 30 min. The reaction was allowed to stir for 4 h while the temperature was maintained at -78 °C, cooling when necessary. To quench the reaction, several crystals of $Na_2SO_4 \cdot 10\ H_2O$ were added at -78 °C. The cold bath was removed, and the reaction mixture was allowed to warm to room temperature.

Dichloromethane (20 mL) was added, followed by anhyd $MgSO_4$ (1g), and the reaction mixture was allowed to stir for 30 mins. The mixture was vacuum filtered and the precipitate was washed with warm 1:1 $CHCl_3$–EtOAc in order to dissolve the aluminum complex formed and until the filtrate was no longer UV active. The solvent was evaporated, and the product was purified by column chromatography eluting with hexane, 3:1 hexane–CH_2Cl_2, and 2:1:1 hexane–CH_2Cl_2–EtOAc. After collection of the desired fractions and after recrystallization from hexane, product **5** (4.12 g, 11.57 mmol, 82.1%) was realized as white crystals.

Physicochemical data: R_f 0.6 (2:1:1 hexane–CH_2Cl_2–EtOAc); ^{1}H NMR data ($CDCl_3$, 300 MHz): δ .95–1.05 and 1.5 (s, 9H, *tert*-butyl), 1.75–2.2 (m, 4H, H-2 and H-3), 1.7–2.1 and 2.5 (s, 1-H), 3.2–3.85 (2dd, 2H, H-5, 4.15–4.4 (m, 1H, H-4), 5.35–5.55 (M-1H, H-1), 7.35–7.75 (m, 10H, phenyl), [Lit.[23] (250 MHz) 1.0 and 1.5 (s, 9H, *tert*-butyl), 1.7–2.2 (m, 4H, H-2 and H-3), 2.0 and 2.4–2.5 (s, 1H, -OH), 3,3–3.9 (2dd, 2H, H-5), 4.1–4.4 (m, 1H, H-4), 5.4–5.6 (m, H, H-1), 7.3, 7.8 (m, 10H, phenyl).

Synthesis of 6-Chloro-9-[5-*O*-(*tert*-butyldiphenylsilyl)-2,3-dideoxy-β-D-*glycero*-pentofuranosyl]purine (6)

5-*O*-*tert*-butyldiphenylsilyl-2,3-dideoxy-D-*glycero*-pentofuranose (**5**, 0.115 g, 0.322 mmol) was massed into a dry round-bottom flask (flask 1) with a stir bar and placed on the pump overnight to insure complete dryness. In a separate flask (flask 2) anhyd K_2CO_3 (0.014 g, 0.10 mmol), benzyltriethylammonium chloride (BTEAC) (0.06 g, 0.26 mmol) and 6-chloropurine (0.06 g, 0.39 mmol) were also placed on the pump overnight. Freshly distilled THF (10 mL) was added to flask 1 and cooled to -78 °C, followed by addition of trifluoroacetic anhydride (TFAA), (0.06 mL, 0.42 mmol) and

pyridine (0.03 mL, 0.4 mmol). The reaction mixture was warmed to -40 °C to -20 °C and allowed to stir for 2 h, cooling when necessary. Anhyd CH_3CN (10 mL) was added to flask 2, and the mixture was cooled to 0 °C using an ice bath. The cold bath was removed from flask 1, and with the aid of a cannula, the reaction mixture was transferred from flask 1 to flask 2. The resulting mixture was slowly warmed to room temperature where it was stirred for an additional 10 h. After evaporation of the solvent, a brown sludge/syrup was left in the flask. After addition of CH_2Cl_2 (25 mL) and stirring for 10 min, vacuum filtration proceeded by high vacuum rotary evaporation, produced a brown residue. Silica gel chromatography was used to purify the residue; a concentration graded eluent was used. Initially 95% petroleum ether to 5% EtOAc was used as the eluent. The concentration of EtOAc was increased by 5% every 100 mL of eluent until the concentration reached 65% pet. ether to 35% EtOAc. Recrystallization from hexane afforded the product **6** (0.136 g, 0.2763 mmol) from which the β-anomer was separated to yield 0.09 g, 0.182 mmol, 56.7%.

Physicochemical data: R_f 0.52 (1:1 hexane–EtOAc); ^{1}H NMR data ($CDCl_3$, 300 MHz): δ 1.05–1.1 (s, 9H, *tert*-butyl), 2.05–2.3 (m, 2H, H-3'), 2.53–2.63 (m, 2H, H-2'), 3.7–4.0 (2dd, 2H, H'5), 4.25–4.35 (m, 1H, H-8), 6.35–6.4 (t, 1H, H-1'), 7.32–7.68 (m, 10H, phenyl), 8.48 (s, 1H, H-8), 8.7 (s, 1H, H-2), [Lit.[23, 24] 1.00–1.1 (s, 9H, *tert*-butyl), 2.05–2.25 (m, 2H, H-3'), 2.5–2.65 (m, 2H, H-2'), 3.7–4.0 (2dd, 2H, H-5'), 4.25–4.4 (m, 1H, H-4'), 6.35–6.42 (t, 1H, H-1'), 7.3–7.70 (m, 10H, phenyl), 8.45 (s, 1H, H-8), 8.7 (s, 1H, H-2)]

Synthesis of 6-Chloro-9-(2,3-dideoxy-β-D-*glycero*-pentofuranosyl)purine (7)

6-Chloro-9-[5-*O*-(*tert*-butyldiphenylsilyl)-2,3-dideoxy-β-D-*glycero*-pentofuranosyl]purine (**6**, 0.2 g, 0.4 mmol) was dissolved in anhyd THF (10 mL), and tetrabutylammonium fluoride TBAF (0.9 mL, 1M THF, 0.89mmol) was added. Next was added triethylamine (TEA, 0.06 g, 0.55 mmol) and HOAc (0.03 g, 0.5mmol) in THF (5 mL) dropwise. This mixture was stirred for 1 h, the solvent was evaporated, and the product was purified on silica gel. The eluent consisted of 58:1 $CHCl_3$–MeOH. Collection and evaporation of the desired fractions yielded (**8**, 0.09 g , 88%) of a white crystalline product after recrystallization from hexane.

Physicochemical data: R_f 0.62 (9:1 CH_2Cl_2–MeOH); ^{1}H NMR data ($CDCl_3$, 300 MHz) 2.15–2.75 (m, 4H, H-2' and H-3'), 3.68–4.08 (2dd, 2H, H-5'), 4.3–4.45 (m, 1H, H-4'), 6.28 (t, 1H), 8.46 (s, 1H), 8.75 (s, 1H), [Lit.[24] 1.95–2.8 (m, 4H), 3.88 (m, 2H), 4.38 (m, 1H), 6.31 (t, 1H), 8.5 (s, 1H), 8.74 (s, 1H)]

List of References

1. Thomas C. Merigan, J.; Bartlett, J. G.; Bolognesi, D. *The Textbook of AIDS Medicine*. 2 ed.; Williams and Wilkins: Baltimore, 1999.
2. Sharma, P. L.; Nurpeisov, V.; Hernandez-Santiago, B.; Beltran, T.; Schinazi, R. F. Nucleoside inhibitors of human immunodeficiency virus type 1 reverse transcriptase. *Curr. Top. Med. Chem.* **2004,** *4*, 895-919.
3. Hutter, M. C.; Helms, V. The mechanism of phosphorylation of natural nucleosides and anti-HIV analogues by nucleoside diphosphate kinase is independent of their sugar substituents. *Chem. Bio. Chem.* **2002,** *3*, 643-651.
4. Schneider, B.; Sarfati, R.; Deville-Bonne, D.; Veron, M. Role of nucleoside diphosphate kinase in the activation of anti-HIV nucleoside analogs. *J. Bioenerg, Biomembr.* **2000,** *32*, 317-324.
5. Lascu, I.; Gonin, P. The catalytic mechanism of nucleoside diphosphate kinases. *J. Bioenerg, Biomembr.* **2000,** *32*, 237-46.
6. Stein, D. S.; Moore, K. H. P. Phosphorylation of nucleoside analog antiretrovirals: a review for clinicians. *Pharmacotherapy* **2001,** *21*, 11-34.
7. Gao, W. Y.; Shirasaka, T.; Johns, D. G.; Broder, S.; Mitsuya, H. Differential phosphorylation and azidothymidine, dideoxycytidine, and dideoxyinosine in resting and activated peripheral blood mononuclear cells. *J. Clin. Invest* **1993,** *91*, 2326-33.
8. Nave, J. F.; Eschbach, A.; Wolff-Kugel, D.; Halazy, S.; Balzarini, J. Enzymatic phosphorylation and pyrophosphorylation of 2',3'-dideoxyadenosine-5'-monophosphate, a key metabolite in the pathway for activation of the anti-HIV (human immunodeficiency virus) agent 2',3'-dideoxyinosine. *Biochem. Pharmacol.* **1994,** *48*, 1105-12.
9. Janin, J.; Dumas, C.; Morera, S.; Xu, Y.; Meyer, P.; Chiadmi, M.; Cherfils, J. Three-dimensional structure of nucleoside diphosphate kinase. *J. Bioenerg, Biomembr.* **2000,** *32*, 215-225.
10. Kreimeyer, A.; Schneider, B.; Sarfati, R.; Faraj, A.; Sommadossi, J. P.; Veron, M.; Deville-Bonne, D. NDP kinase reactivity towards 3TC nucleotides. *Antivir. Res.* **2001,** *50*, 147-156.
11. Bourdais, J.; Biondi, R.; Sarfati, S.; Guerreiro, C.; Lascu, I.; Janin, J.; Veron, M. Cellular phosphorylation of anti-HIV nucleosides. Role of nucleoside diphosphate kinase. *J. Biol. Chem.* **1996,** *271*, 7887-90.
12. Anderson, B. D.; Morgan, M. E.; Singhal, D. Enhanced oral bioavailability of DDI after administration of 6-Cl-ddP, an adenosine deaminase-activated prodrug, to chronically catheterized rats. *Pharma. Res.* **1995,** *12*, 1126-33.
13. Price, R. W.; Brew, B. J. The AIDS dementia complex. *J. Infect. Dis.* **1988,** 158, 1079-83.

14. Anderson, B. D.; Hoesterey, B. L.; Baker, D. C.; Galinsky, R. E. Uptake kinetics of 2',3'-dideoxyinosine into brain and cerebrospinal fluid of rats: intravenous infusion studies. *J. Pharmacol. Exper. Therapeuti.* **1990,** *253*, 113-18.
15. Azizbigloo, F. Synthesis of Sterically Hindered 5'Esters if 6-Chloro-9-(2,3-dideoxy-beta-D-Glycero-pentofuranosyl)purine as Anti-HIV Agents. The University of Tennessee, Knoxville, 1997.
16. Morgan, M. E.; Chi, S. C.; Murakami, K.; Mitsuya, H.; Anderson, B. D. Central nervous system targeting of 2',3'-dideoxyinosine via adenosine deaminase-activated 6-halo-dideoxypurine prodrugs. *Antimicrob. Agents. Chemother.* **1992,** *36*, 2156-65.
17. Cervoni, L.; Lascu, I.; Xu, Y.; Gonin, P.; Morr, M.; Merouani, M.; Janin, J.; Giartosio, A. Binding of nucleotides to nucleoside diphosphate kinase: A calorimetric study. *Biochemistry* **2001,** *40*, 4583-4589.
18. Chen, Y.; Gallois-Montbrun, S.; Schneider, B.; Veron, M.; Morera, S.; Deville-Bonne, D.; Janin, J. Nucleotide Binding to Nucleoside Diphosphate Kinases: X-ray Structure of Human NDPK-A in Complex with ADP and Comparison to Protein Kinases. *J. Mol. Biol.* **2003,** *332*, 915-926.
19. Austin, A. T.; Howard, J. Reaction of HNO_2 with glutamine and glutamic acid. *J. Chem. Soc.* **1961**, 3593-3603.
20. Brown, H. C.; Rao, B. C. S. Hydroboration. III. The reduction of organic compounds by diborane, an acid-type reducing agent. *J. Am. Chem. Soc.* **1960,** *82*, 681-6.
21. Chaudhary, S. K.; Hernandez, O. 4-Dimethylaminopyridine: an efficient and selective catalyst for the silylation of alcohols. *Tetrahedron Lett.* **1979**, 99-102.
22. Uzi Ravid, R. S., Leverett Smith. Synthesis of the Enantiomers of 4-substituted Gamma Lactones with Known Absolute Configuration. *Tetrahedrom* **1977,** *34*, 1448-1452.
23. Azizbigloo, F. Synthesis of Sterically Hindered 5'-Esters of 6-Chloro-9-(2,3-Dideoxy-beta-D-Glycero-Pentofuranosyl Purine as Anti-HIV Agents. Tennessee, Knoxville, 1997.
24. Chu, C. K.; Ullas, G.; Lak, J. Synthesis and Structure-Activity Relationships of 6-Substituted 2',3'-Dideoxypurine Nucleosides as Potential Anti-Human Immunodeficiency Virus Agents. *J. Med. Chem.* **1990,** *33*, 1553-1561.

APPENDIX

^{1}H NMR Spectra

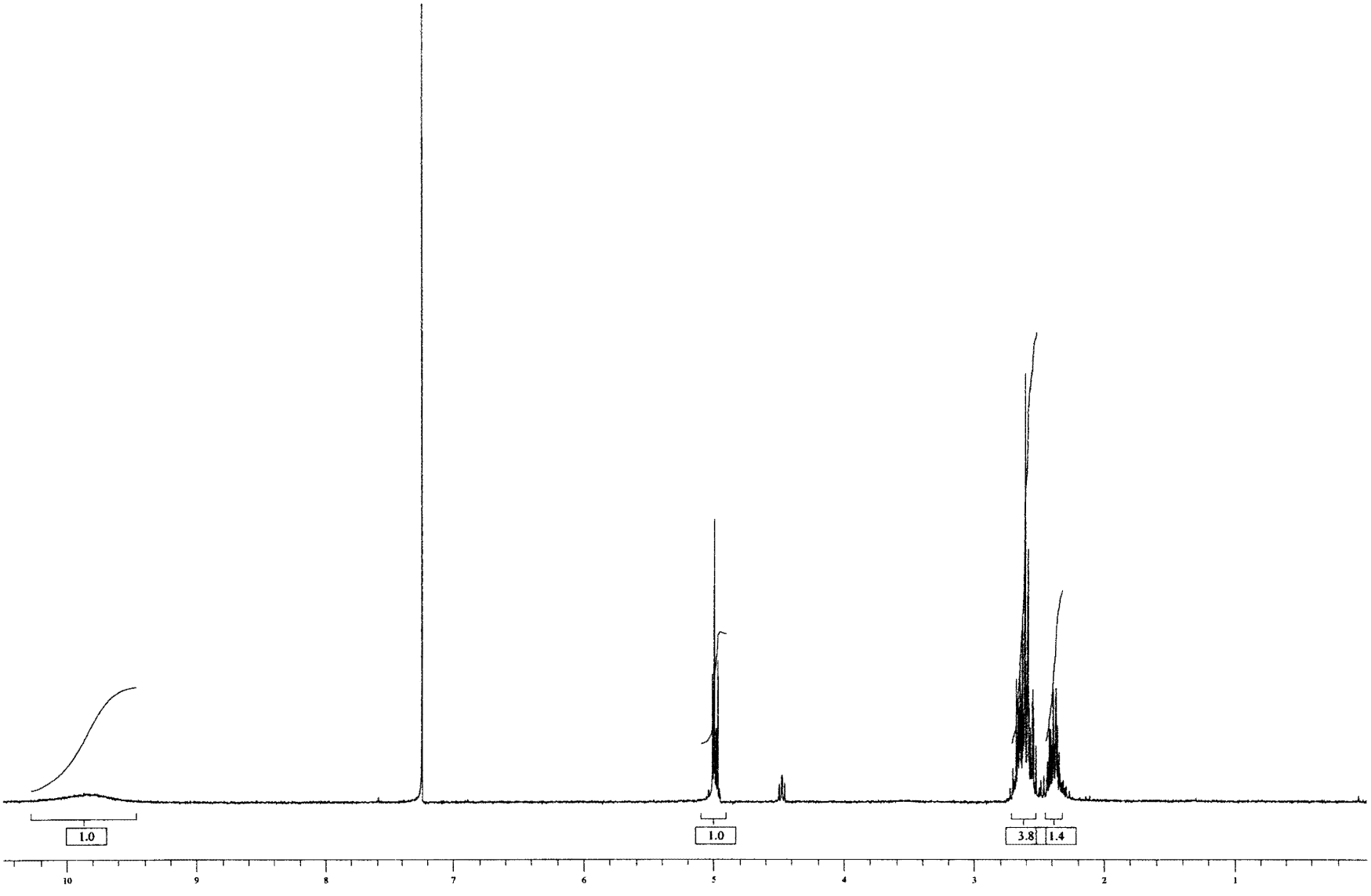

^{1}H NMR ($CDCl_3$, 300 MHz) Spectrum of (S)-γ-Carboxy-γ-butyrolactone (**2**)

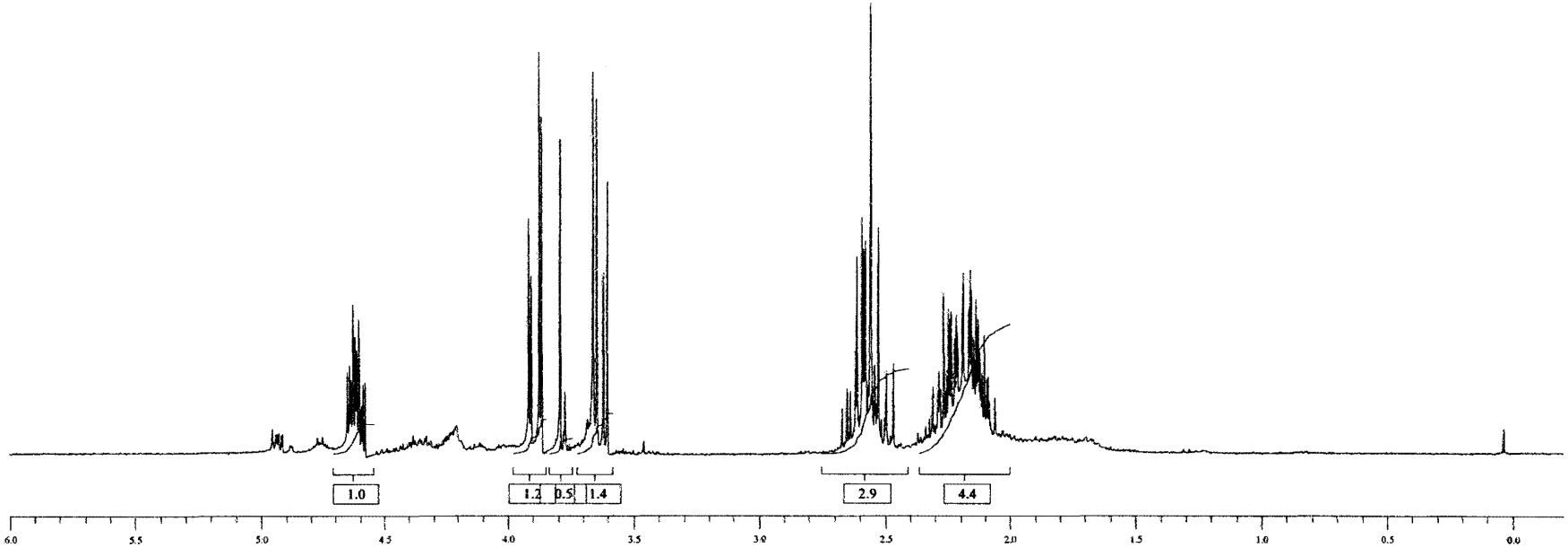

^{1}H NMR ($CDCl_3$, 300MHz) Spectrum of (S)-(+)-Hydroxymethyl-γ-butyrolactone (**3**)

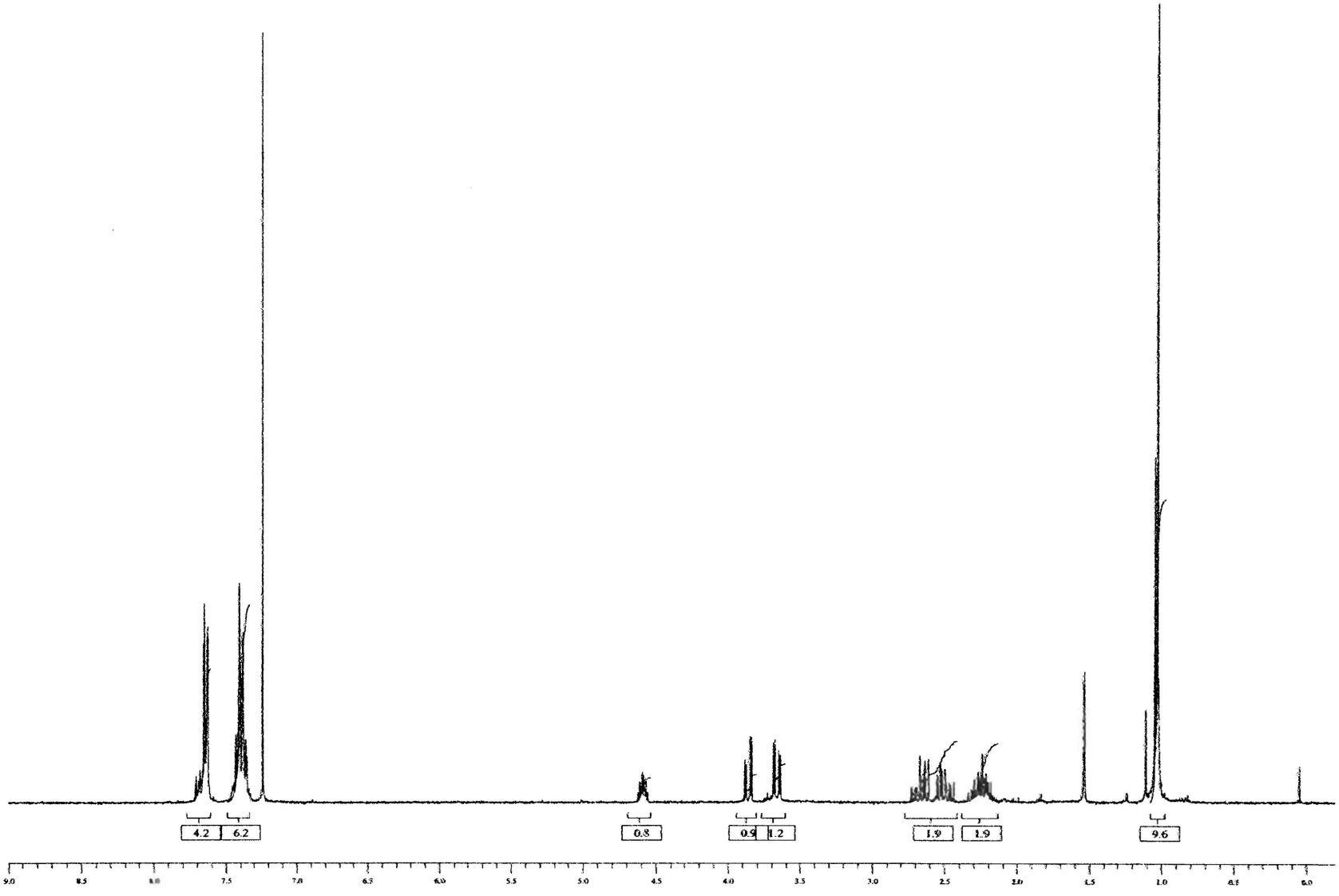

^{1}H NMR ($CDCl_3$, 300 MHz) Spectrum of S-(+)-tert-Butyldiphenylsilyloxymethyl-γ-butyrolactone (4)

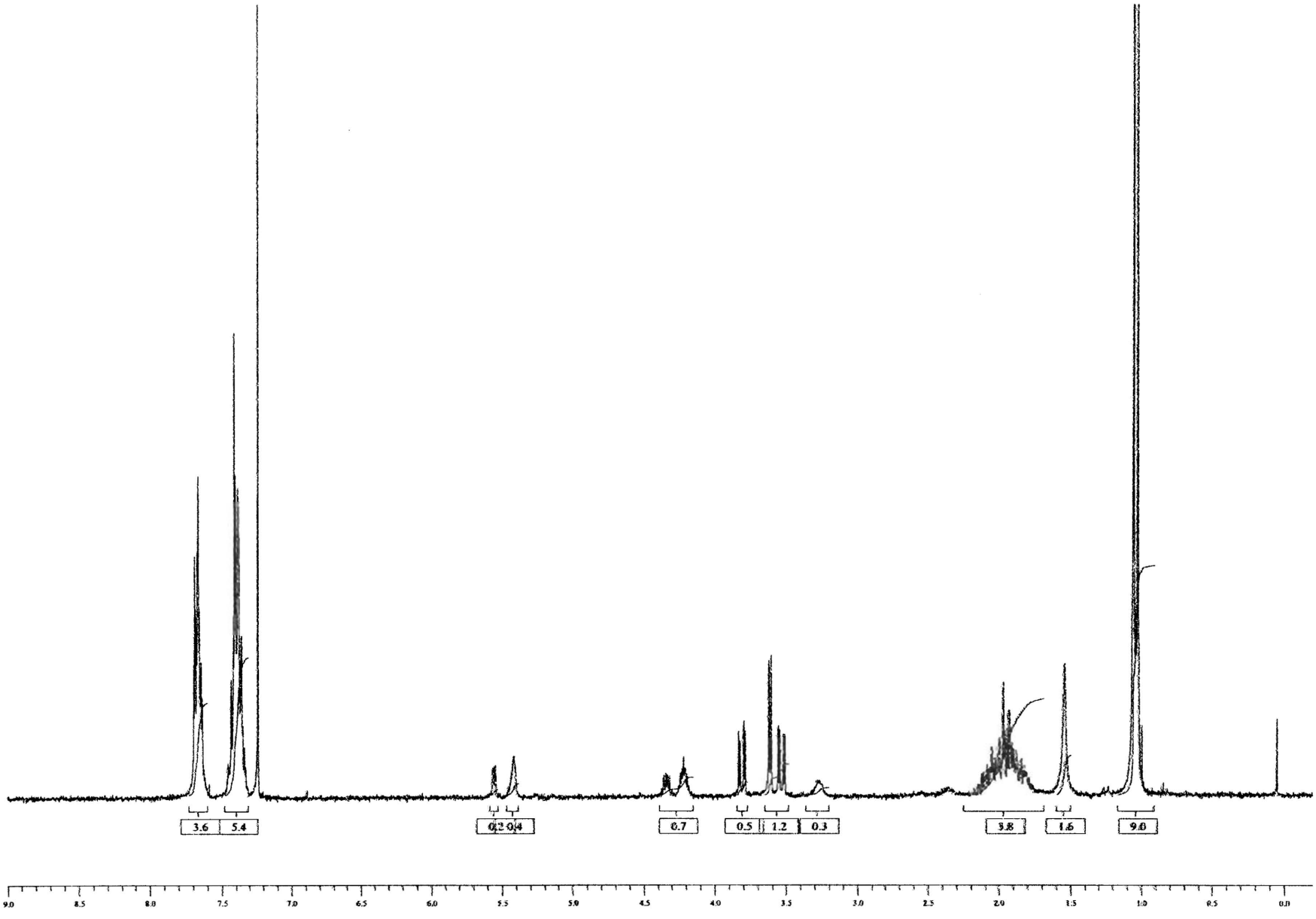

^{1}H NMR ($CDCl_3$, 300 MHz) Spectrum of 5-O-tert-butyldiphenylsilyl-2,3-dideoxy-D-glycero-pentofuranose **(5)**

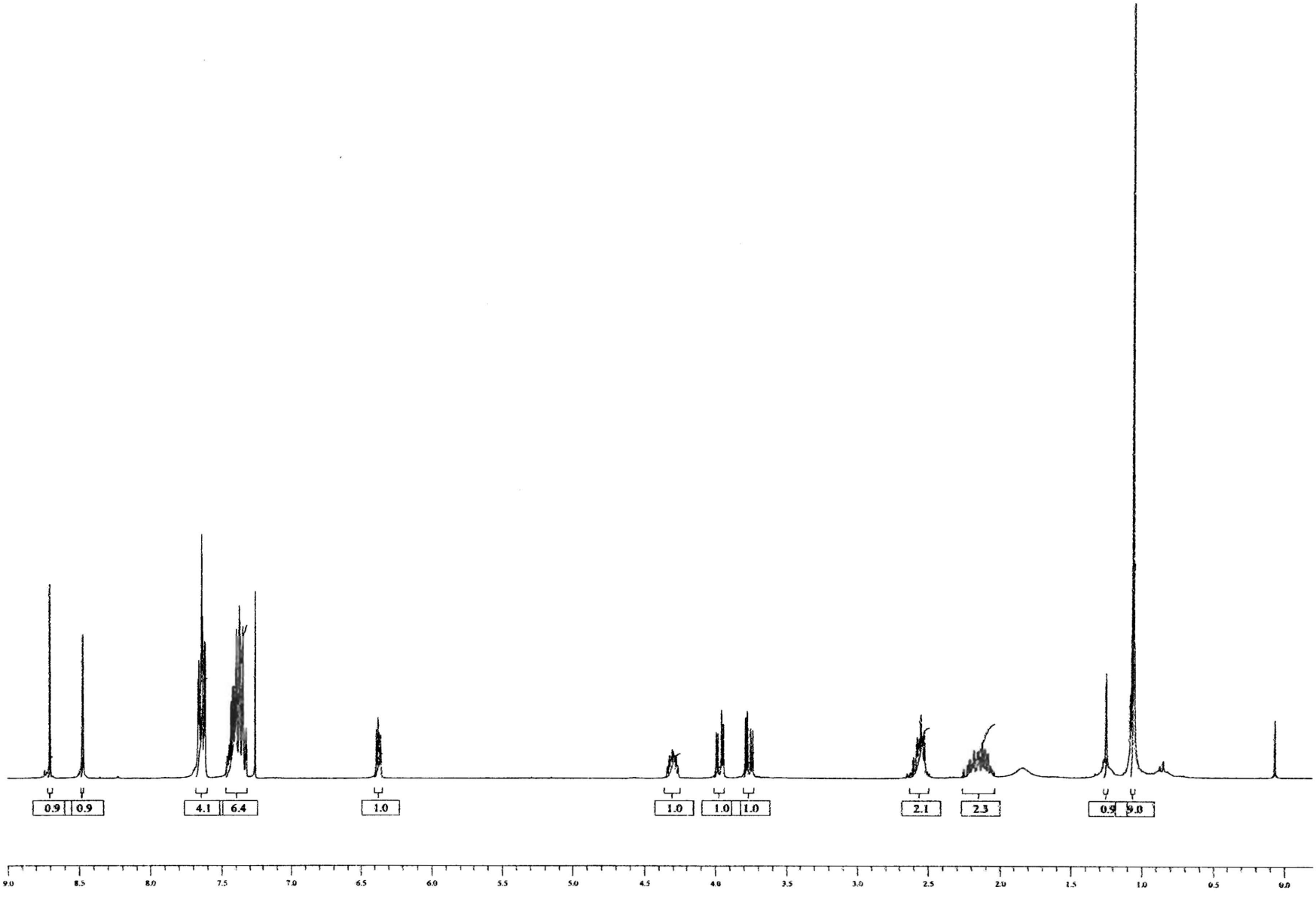

^{1}H NMR ($CDCl_3$, 300 MHz) Spectrum of 6-Chloro-9-[5-O-(tert-butyldiphenylsilyl)-2,3-dideoxy-β-D-glycero-pentofuranosyl]purine **(6)**

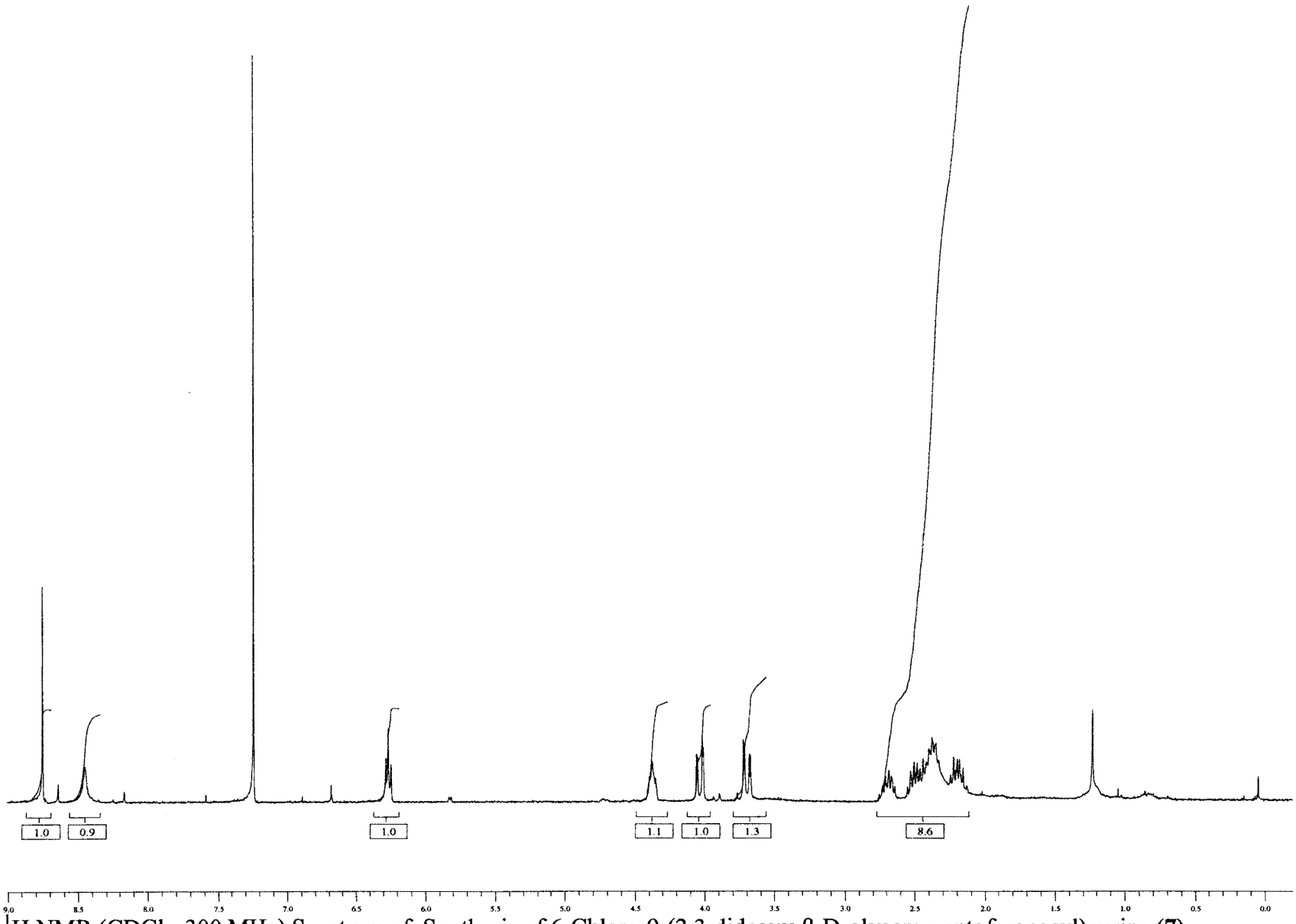

^{1}H NMR ($CDCl_3$, 300 MHz) Spectrum of Synthesis of 6-Chloro-9-(2,3-dideoxy-β-D-glycero-pentofuranosyl)purine (**7**)